Gene Expression Patterns 44 (2022) 119246

Contents lists available at ScienceDirect

Gene Expression Patterns

journal homepage: www.elsevier.com/locate/gep

A new transgenic reporter line reveals expression of protocadherin 9 at a cellular level within the zebrafish central nervous system

Judith Habicher [a], Remy Manuel [a], Andrea Pedroni [b], Charles Ferebee [a], Konstantinos Ampatzis [b], Henrik Boije [a,*]

[a] Department of Neuroscience, Uppsala University, Uppsala, Sweden
[b] Department of Neuroscience, Karolinska Institutet, Stockholm, Sweden

A B S T R A C T

The wiring of neuronal networks is far from understood. One outstanding question is how neurons of different types link up to form subnetworks within the greater context. Cadherins have been suggested to create an inclusion code where interconnected neurons express the same subtypes. Here, we have used a CRISPR/Cas9 knock-in approach to generate a transgenic zebrafish reporter line for protocadherin 9 (*pcdh9*), which is predominantly expressed within the central nervous system. Expression of eGFP was detected in subsets of neurons in the cerebellum, retina and spinal cord, in both larvae and juveniles. A closer characterization of the spinal locomotor network revealed that a portion of distinct classes of both excitatory and inhibitory interneurons, as well as motor neurons, expressed *pcdh9*. This transgenic line could thus be used to test the cadherin network hypothesis, through electrophysiological characterization of eGFP positive cells, to show if these are synaptically connected and form a discrete network within the spinal cord.

1. Introduction

Cellular communication is key during organ development and an array of proteins enable cell-to-cell interactions to form complex structures such as the nervous system. The protocadherins (pcdhs), a cadherin superfamily subgroup of some 80 proteins, regulate cell contacts through homophilic interactions and are expressed in distinct spatio-temporal patterns in the central nervous system (Frank and Kemler, 2002; Peek et al., 2017). It has been hypothesized that pcdhs act as a molecular inclusion code, as neurons connected in the same neuronal network often express the same subtypes (Vanhalst et al., 2005).

Here we focused on protocadherin 9 (*pcdh9*), a member of the δ1-Protocadherin subfamily, involved in establishing and disrupting cell adhesion, a dual role thought to rely on co-receptors (Vanhalst et al., 2005; Peek et al., 2017). The δ1-protocadherins predominantly localize perisynaptical in axons and dendrites and have been associated with regulating dendritic initiation, growth, morphology, arbor refinement, and spine formation (Pancho et al., 2020). Studies in chick (Lin et al., 2012), mice (Asahina et al., 2012), and zebrafish (Liu et al., 2009) show that *pcdh9* is predominantly expressed in the brain and spinal cord but technical limitations prevented analysis at a cellular level.

For a detailed overview of *pcdh9* expression, we generated a transgenic zebrafish reporter line, *Tg*(*pcdh9*:hs:eGFP), through CRISPR/Cas9-mediated knock-in (Kimura et al., 2015). High-resolution images revealed expression of *pcdh9* at a cellular level within the brain and spinal cord. By combining *Tg*(*pcdh9*:hs:eGFP) with other transgenic reporter lines or immunohistochemistry, we present a detailed description of *pcdh9* positive cells in structures such as the cerebellum, pineal gland, retina, and spinal cord. A more extensive analysis of the spinal cord suggests that *pcdh9* is expressed in multiple cell types of the locomotor network. Our characterization of the transgenic reporter line provides a stepping-stone for testing the hypothesis that these cells, which share the same protocadherin, are part of the same subnetwork. Future studies, employing electrophysiological characterization of *pcdh9* positive cells, could give insights into how substructures are formed and connected within the nervous system.

2. Results and discussion

We set out to characterize the expression of *pcdh9* during zebrafish development using an eGFP reporter line generated through CRISPR/Cas9-mediated knock-in (Fig. 1A). By PCR and sequencing, we confirmed the position and direction of the eGFP insert in the zebrafish genome. Overview imaging of larvae during development revealed eGFP expression in the brain, eye, and spinal cord (Fig. 1B and C).

* Corresponding author.
E-mail address: henrik.boije@neuro.uu.se (H. Boije).

https://doi.org/10.1016/j.gep.2022.119246
Received 16 December 2021; Received in revised form 7 March 2022; Accepted 9 April 2022
Available online 12 April 2022

2.1. Expression of pcdh9:hs:eGFP in the brain and eye

In the brain, eGFP positive cells were found in the forebrain, midbrain and hindbrain, and the fluorescence reporter became more apparent as development progressed. At 1 day post fertilisation (dpf) the expression in the brain was apparent in the antereoventral forebrain and in the ventral hindbrain (Supplementary Fig. 1), as previously shown using *in situ* hybridization (Liu et al., 2009). At 3 dpf we could identify distinct eGFP positive cells in the optic tectum (TeO), the cerebellum (CCe), the hindbrain (Hb), the epiphysis (E) as well as in the retina (Fig. 2A and B). This expression pattern is supported by a previous characterization of *pcdh9* expression using *in situ* hybridization (Liu et al., 2009). Next, we characterized cells labelled in *Tg*(*pcdh9*:hs:eGFP) larvae by combining them with other transgenic lines or through immunohistochemistry.

2.1.1. Cerebellum: Purkinje cells express pcdh9

Purkinje cells, the principal neurons of cerebellar computations, play a key role in the dynamic formation of the internal models of the cerebellum (Medina, 2011). In zebrafish, differentiated Purkinje cells are found already at 3 dpf (Hamling et al., 2015). We classified *pcdh9* positive cells in the cerebellum as Purkinje cells based on their morphology (Fig. 2C). To further characterize these cells, we crossed *Tg*(*pcdh9*:hs:eGFP) with *Tg*(*ptf1a*:dsRed); a gene crucial for the generation of inhibitory interneurons, such as the Purkinje cells in the cerebellum (Sellick et al., 2004; Hoshino et al., 2005; Jusuf and Harris, 2009a). We found double labelled cells at 5 dpf, but there were also *pcdh9* positive cells that did not express *ptf1a* (Fig. 2C).

2.1.2. Ear: axons projecting to hair cell clusters are positive for pcdh9

The zebrafish inner ear has five sensory patches, three of which are cristae (Nicolson, 2005). We crossed *Tg*(*pcdh9*:hs:eGFP) with *Tg*(*HuC*:GAL4; UAS:RFP), which labels both neurons and hair cells (Wada et al., 2013; Iwasaki et al., 2020). We observed *pcdh9*:hs:eGFP positive axons that terminated at the level of the hair cells in the anterior, medial, and posterior crista of the inner ear (Fig. 2D). However, due to the vast number of cells in the brain, we could not trace these axons back to their cell bodies. It should also be noted that we did not observe *pcdh9* positive axons to the hair cells of the anterior or posterior lateral line, but instead observed cells surrounding the afferent ganglion cells and axons to the lateral line in a glial manner (Xiao et al., 2015).

2.1.3. Epiphysis: photoreceptor cells express pcdh9

In the diencephalon, *pcdh9*:hs:eGFP positive cells were located at the level of the epiphysis (Fig. 2E), previously described in an *in situ* study (Liu et al., 2009). The zebrafish epiphysis consists of three main cell types: photoreceptor cells, projection neurons, and interstitial cells (Shainer et al., 2017). We attempted to correlate *pcdh9* expression to these cell types via antibody staining against Isl1, which is expressed in both pineal photoreceptors and projection neurons (Masai et al., 1997). At 3 dpf, all pineal *pcdh9*-eGFP cells were also stained for Isl1 (Fig. 2E). Although this excluded the interstitial cells, it did not allow us to distinguish between photoreceptors and projection neurons. Still, based on morphological characteristics (*i.e.* large soma, distinct projections (Li et al., 2012)), we were able to identify part of *pcdh9*:hs:eGFP positive cells as double-cone photoreceptor cells.

2.1.4. Eye: a subset of ganglion, amacrine and bipolar cells are pcdh9 positive in the retina

Analysis of the eye revealed that *e*GFP positive cells were located in the ganglion cell layer (GCL) and the inner nuclear layer (INL) of the zebrafish retina (Fig. 2F), where the latter consists of bipolar, horizontal, and amacrine cells (Iribarne, 2020). To gain further insight into the identity of these eGFP positive cells, we crossed *Tg*(*pcdh9*:hs:eGFP) with *Tg*(*ptf1a*:dsRed), which labels amacrine and horizontal cells in the INL (Jusuf and Harris, 2009b; Boije et al., 2016). We found eGFP positive

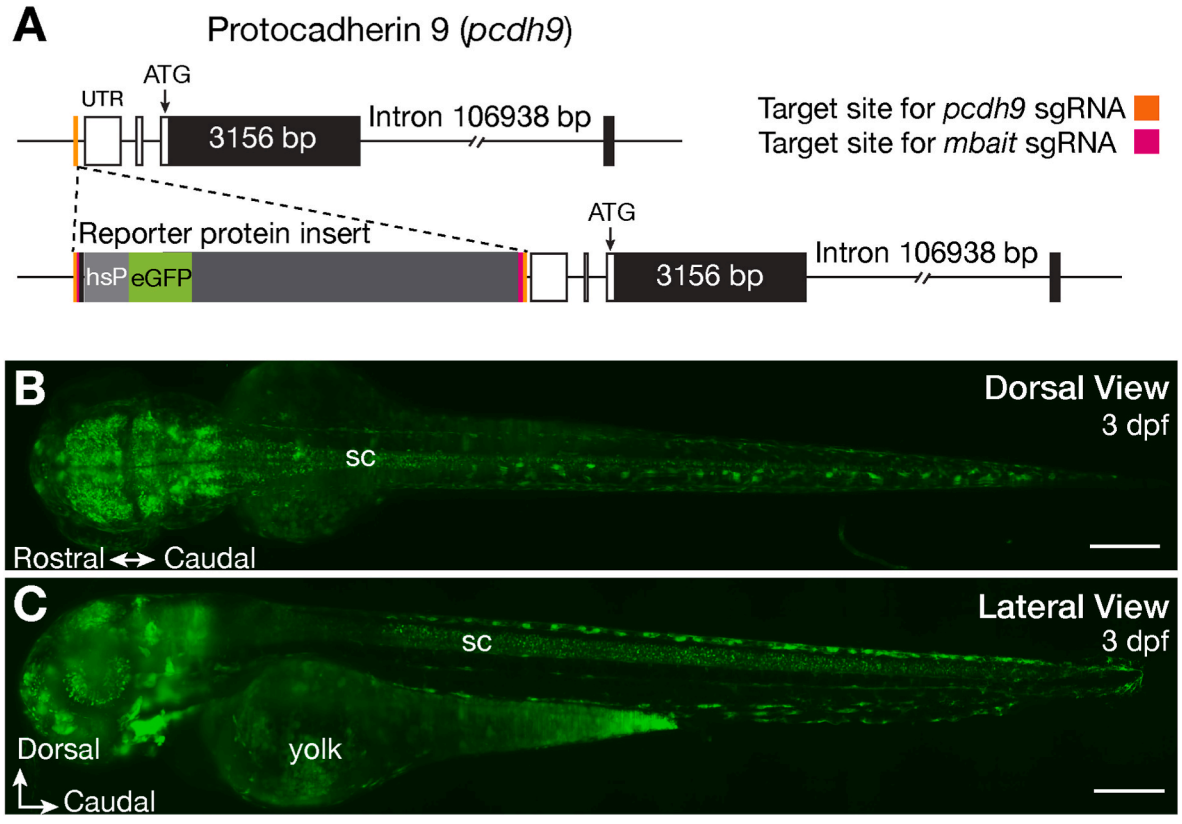

Fig. 1. Generation of a *pcdh9*:hs:eGFP reporter line. Targeted genomic integration of the eGFP reporter construct (A) and overview of eGFP expression in Tg(*pcdh9*:hs:eGFP) larvae at 3 days post fertilisation (dpf) in a dorsal (B) and lateral (C) view of the brain and spinal cord (sc). Scale bars equal 200 μm.

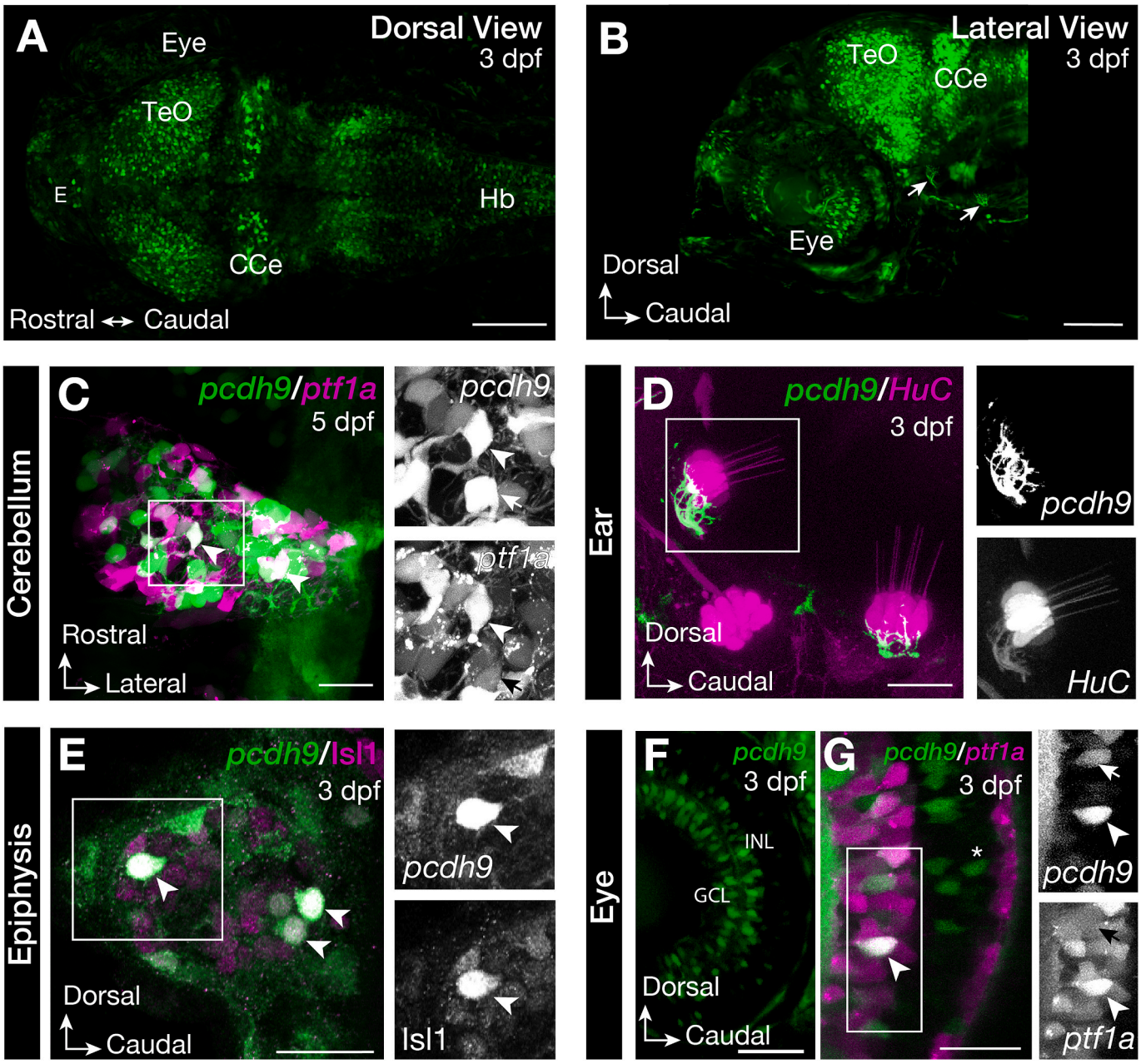

Fig. 2. Tg(*pcdh9*:hs:GFP) expression in the brain of zebrafish larvae. Dorsal (A) and lateral view (B) of the brain of Tg(*pcdh9*:hs:GFP) zebrafish at 3 days post fertilisation (dpf) show expression in the optic tectum (TeO), cerebellum (CCe), epiphysis (E), in the retina of the eye, the hindbrain (Hb) and axons connecting to the hair cells of the ear (arrow). In the cerebellum *pcdh9* was expressed in a subpopulation of Purkinje cells labelled by Tg(*ptf1a*:dsRed) (arrowhead), *ptf1a* negative cells are indicated with an arrow (C). In the ear, *pcdh9* positive axons connecting to the hair cells, labelled by Tg(*HuC*:GAL4; UAS:RFP), were observed (D). Immunohistochemistry showed that all *pcdh9*-eGFP positive cells in the epiphysis were positive for Isl1 (E). The *pcdh9*-eGFP positive cells in the retina were located in the ganglion cell layer (GCL) and in the inner nuclear layer (INL) (F). In the INL a subset of *pcdh9* positive cells were amacrine cells labelled by Tg(*ptf1a*:dsred) (arrowhead), a subset negative for *ptf1a* (arrows). Bipolar cells were also *pcdh9* positive (G, asterix). Scale bars equal 100 μm in A-B and 20 μm in C-G.

cells that overlapped with *ptfa1*:dsRed in the INL, corresponding to the position of the amacrine cells (Fig. 2G). Several *ptfa1*:dsRed cells were negative for *pcdh9*:hs:eGFP, indicating that *pcdh9* is expressed only in a subset of the amacrine cells. No *pcdh9* expression was found in the INL at the level of the horizontal cells. In addition, we identified *pcdh9*:hs:eGFP cells that were negative for *ptf1a*:dsRed, situated between amacrine and horizontal cells, suggesting that they were bipolar cells (Fig. 2G). eGFP positive cells in the GCL were negative for *ptf1a*:dsRed indicating that they were indeed ganglion cells and not displaced amacrine cells. In addition, we examined expression patterns in zebrafish at 21 dpf and found eGFP positive amacrine cells as well as elaborate projections in the inner plexiform layer (Supplementary Fig. 2).

The observation that a limited number of retinal cells of different subtypes express *pcdh9* within this local circuit gives credit to the hypothesis that *pcdh9*-expressing cells may form a subnetwork. To build on this idea, we performed a more detailed analysis of the cells labelled in the spinal cord, where speed-dependent subnetworks have been described through functional analysis (Ampatzis et al., 2013).

2.2. Expression of pcdh9:hs:eGFP in the spinal cord

The spinal locomotor network consists of sets of excitatory and inhibitory interneurons, which drive the rhythmic output through motor neurons, and are modulated by input from sensory neurons located in the dorsal root ganglia (DRG) (Berg et al., 2018). Throughout the spinal cord, we found numerous *pcdh9*:hs:eGFP positive cells at 3 dpf (Fig. 3A,B and S1, S2, S3 Movie). The cells are distributed across the ventral-dorsal and the medial-lateral axis. Based on the spatial distribution of *pcdh9* positive cells, we hypothesized that our population consists of several neuronal types within the locomotor network. To characterize the nature of these *pcdh9*-expressing cells, we crossed Tg (*pcdh9*:hs:eGFP) with different transgenic reporter lines marking motor neurons or locomotor-related interneuron subpopulations. In addition, we performed antibody staining to label neuronal populations for which we lacked transgenic lines.

2.2.1. Sensory neurons: the dorsal root ganglia express pcdh9

Dorsal root ganglia are located outside the spinal cord and contain the nuclei of peripheral sensory neurons, which convey information regarding touch, perception of pain (nociception), temperature, and sense of limb movement and position (proprioception) to the central nervous system (McGraw et al., 2008). During zebrafish development, the amount of DRG cells have been quantified over time. Between 3 and 6 dpf there are approximately five cells in a single DRG and at 20 dpf this has increased to around 30 cells (McGraw et al., 2008; McGraw et al., 2012). In Tg(*pcdh9*:hs:eGFP) larvae, we identified 1–3 *pcdh9* positive cells per DRG at 3–6 dpf, where a single cell was the most frequent observation (Fig. 3C). When we assessed the number of *pcdh9* positive cells in the DRG at 19 dpf, we could identify up to 10 cells (Fig. 3D). This indicates that only a subset of DRG cells express *pcdh9*. Using an antibody against Isl1, which is expressed in DRG cells, we could see co-expression (Fig. 3E). The presence of *pcdh9* expressing neurons in the DRG is in line with previous findings in mice (Asahina et al., 2012) and chicken (Lin et al., 2012).

The zebrafish has two types of sensory neurons with their somas positioned in the spinal cord: the Rohon Beard neurons, mechanosensory cells that project into the periphery, and the Kolmer–Agdur cells (or CFS-cNs), which regulate proprioception within the spinal cord (Henderson et al., 2019). Rohon Beard neurons have large somas located medial and dorsal in the spinal cord and express Isl1 (Lencer et al., 2021). By immunohistochemistry we could identify the Rohon Beard cells but found no overlap with the *pcdh9*:hs:eGFP positive cells (Fig. 3F). Unfortunately, we lacked a good marker to identify the CSF-cnS cells within the spinal cord of Tg(*pcdh9*:hs:eGFP), and could therefore not confirm nor exclude the expression of *pcdh9* in these neurons.

2.2.2. Glia: cells ensheathing motor neuron axons are pcdh9 positive

Imaging of DRG neurons revealed labelled cells outside the ventral spinal cord (Fig. 3G). By crossing the Tg(*pcdh9*:hs:eGFP) fish with Tg (*mnx1*:Gal4; UAS:RFP), a marker for motor neurons (Seredick et al., 2012; Bello-Rojas et al., 2019), we could show that the *pcdh9* positive cells surrounded motor neuron axons in a glial manner (Fig. 3G). Without specific markers, we were unable to identify the type of glia but possible candidates are the perineurial glia cells, which play an important role in axon guidance of motor neurons (Morris et al., 2017) and the Motor Exit Point (MEP) glia, which bridges the myelin of the periphery and central nervous system (Fontenas and Kucenas, 2018).

2.2.3. Motor neurons: secondary motor neurons express pcdh9

We were unable to detect obvious axon bundles leaving the spinal cord in *Tg*(*pcdh9*:hs:eGFP) larvae, possibly due to the overlap with *pcdh9* positive glia cells. In order to explore if motor neurons were eGFP positive we examined *Tg*(*pcdh9*:hs:eGFP), *Tg*(*mnx1*:Gal4; UAS:RFP) double transgenic larvae. This revealed co-expression at 3 dpf, indicating that a number of motor neurons in each segment were positive for *pcdh9* (Fig. 3H). Based on their soma size and position within the spinal cord, we mainly identified secondary motor neurons among the double-labelled cells (Fig. 3H).

2.2.4. Interneurons: both inhibitory and excitatory interneurons are pcdh9 positive

Over 20 types of interneurons have been classified in the spinal cord based on their electrophysiological output, gene expression and morphology (Hale et al., 2001; Alaynick et al., 2011). We explored the co-expression of a number of markers, unique for different subpopulations of interneurons, with the expression of *pcdh9*. Following immunohistochemistry against Evx2, a marker for the excitatory V0 population of interneurons (Moran-Rivard et al., 2001), we observed eGFP, Evx2 double positive cells (Fig. 3I). Next, we crossed *Tg*(*pcdh9*:hs:eGFP) with *Tg*(*dmrt3*:Gal4; UAS:RFP), a marker for a subpopulation of dI6 interneurons (Andersson et al., 2012), and found double positive cells (Fig. 3J). In addition, antibody staining against Wt1a, a marker for another subpopulation of dI6 interneurons (Goulding, 2009), revealed co-expressing cells (Fig. 3K). This expression of *pcdh9* in dI6 neurons have previously been observed in a single cell RNA sequencing analysis (Iglesias Gonzalez et al., 2021). All three populations of interneurons, *i.e. evx2*, *dmrt3a*, and *wt1a*, showed expression of *pcdh9* in a select few cells within their respective populations. Interestingly, a fourth marker used, *ptf1a*, which labels inhibitory neurons from the di4/DiL lineage involved in sensory processing (Comer et al., 2015), did not reveal any overlap with eGFP (Fig. 3L).

Although our data does not allow us to make conclusions on direct connections between labelled cells, our efforts to identify the cell types labelled within the spinal cord do not discourage such a possibility. The spinal locomotor network in zebrafish contains a number of neurons: excitatory interneurons (shown by *evx2*), inhibitory interneurons (shown by *dmrt3a/wt1a*), and motor neurons (shown by *mnx1*).

2.3. Expression of pcdh9 in juvenile zebrafish

The expression of *pcdh9*:hs:eGFP was verified in the spinal cord and in the cerebellum of juvenile zebrafish. In the spinal cord, distinct eGFP positive cells were identified in the most ventral and lateral portion of each segment (Fig. 4A). To verify that *pcdh9* positive cells were neurons, we used immunohistochemistry against the pan-neuronal marker HuC/D. All eGFP-positive cells were also positive for HuC/D, indicating that *pcdh9* is expressed in a small population of neurons in the juvenile spinal cord (Fig. 4A). To further characterize the identity of *eGFP* positive neurons we performed retrograde labelling of motor neurons by biotinylated dextran dye injection into the muscles (Ampatzis et al., 2013). Notably, only a small proportion of motor neurons showed colocalization with eGFP positive cells and based on their soma size and position within the spinal cord, they were identified as motor neurons belonging to the slow circuitry (Ampatzis et al., 2013) (Fig. 4B and C).

pcdh9 positive cells were identified in the corpus cerebelli (CCe) and in the valvula medialis (Vam) and lateralis (Val). ZebrinII, a marker for Purkinje cells (Bae et al., 2009), revealed a partial overlap, but there were also *pcdh9* positive and ZebrinII negative cells. Due to the layered organization of the cerebellum these cells could potentially be Eurydendroyd cells, indicating that *pcdh9* is expressed in a mixed subpopulation of Purkinje and Eurydendroyd cells, in both the corpus and in the valvular cerebelli (Fig. 4D and E).

3. Conclusion

There is a range of cell types positive for *pcdh9* in the zebrafish nervous system. Our data corroborates previous characterizations but this new transgenic reporter line enables a test of the network hypothesis. The speed-dependent circuits of the zebrafish locomotor network consist of three distinct modules, each built up by excitatory and

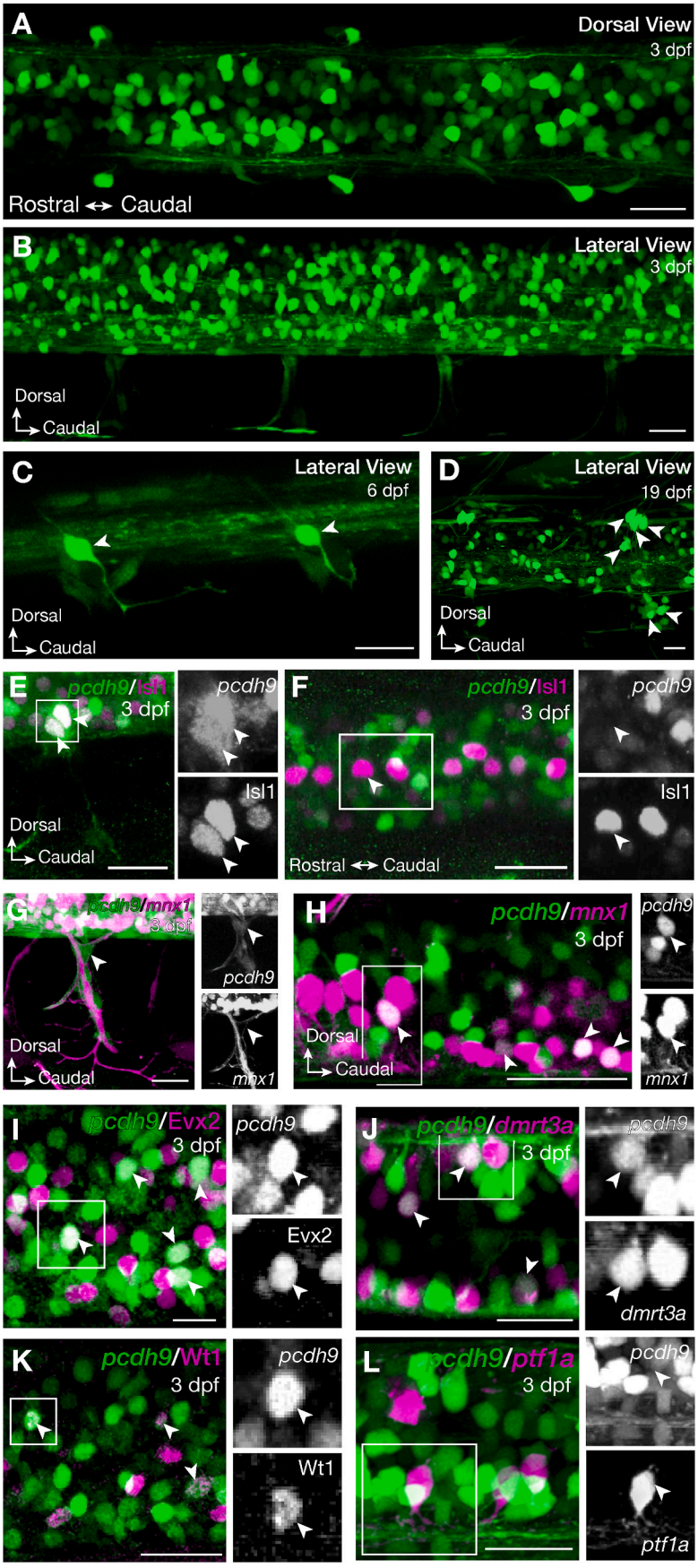

Fig. 3. Tg(*pcdh9*:hs:GFP) zebrafish larvae in the zebrafish spinal cord. Dorsal (A) and lateral view (B) of the spinal cord of Tg(*pcdh9*:hs:GFP) zebrafish at 3 days post fertilisation (dpf) showed *pcdh9* positive cells within and outside the spinal cord. One cell of the dorsal root ganglia per hemi-segment was *pcdh9* positive at 6 dpf (C; arrowhead) and up to 10 cells per hemi-segment were labelled at 19 dpf (D; arrowheads). These cells were Isl1 positive (E). Isl1 also stains the Rohon Beard cells, which were negative for *pcdh9* (F). Crossing Tg(*pcdh9*:hs:eGFP) with Tg(*mnx1*:Gal4; UAS:RFP) revealed the *pcdh9* positive glia cells encasing the motor neuron axons leaving the spinal cord (G) and overlap of *mnx1* and *pcdh9* expressing cells in secondary motor neurons (H; arrowhead). Immunohistochemistry for Evx2 revealed overlap with *pcdh9*-eGFP positive interneurons in the spinal cord (I). Expression of *pcdh9* was also observed in the dI6 interneurons marked by *dmrt3a* (Tg(*dmrt3a*:GAL4; UAS:RFP)) (J) or Wt1 (immunohistochemistry) (K), but not in the dI4 interneurons labelled by (Tg(*ptf1a*:dsred) (L). Scale bars equal 20 μm.

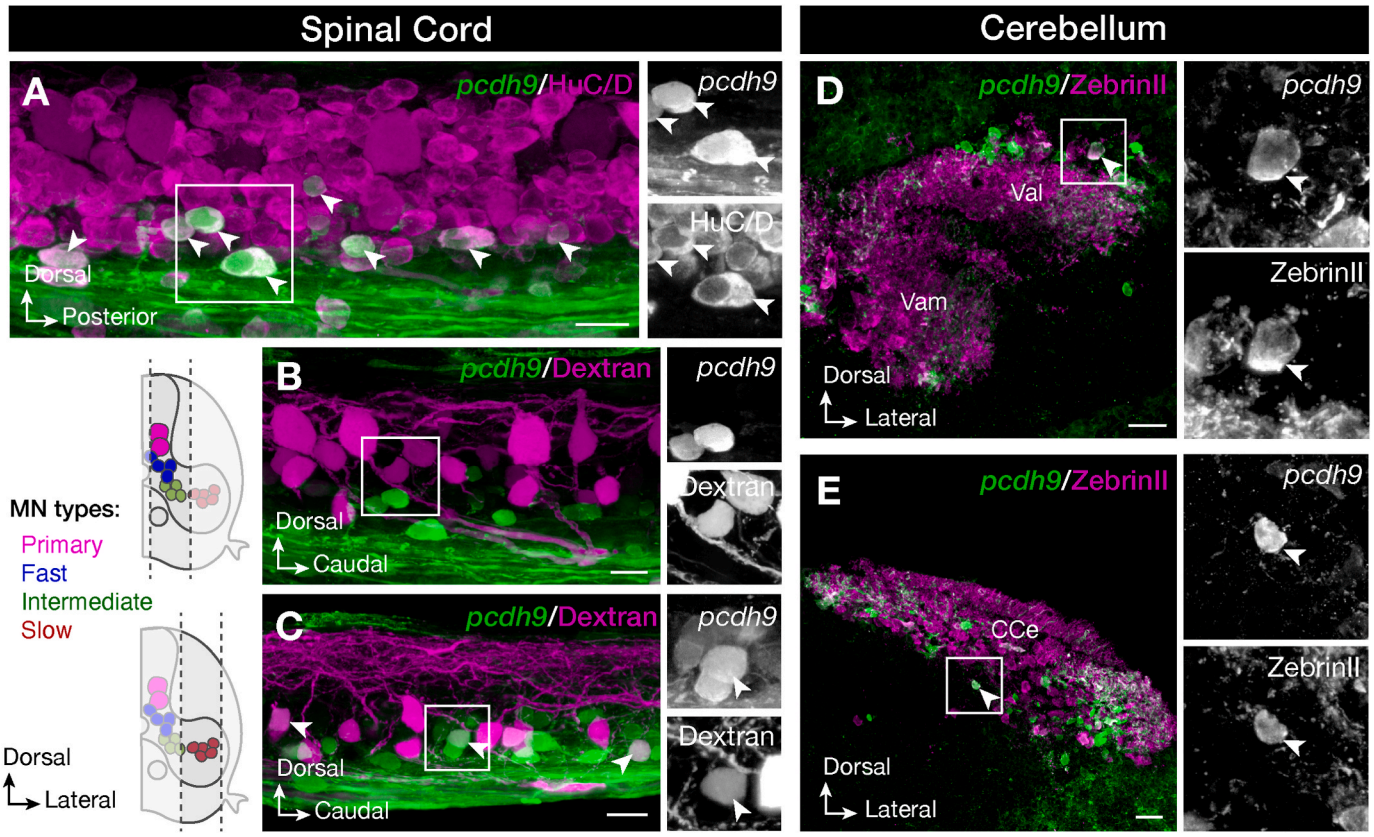

Fig. 4. Tg(*pcdh9*:hs:GFP) juvenile zebrafish exhibit expression both in the spinal cord and in the cerebellum. All the *pcdh9* positive cells expressed the pan-neuronal marker HuC/D (A). Retrograde labelling of motor neurons showed a specific expression of *pcdh9* in a portion of slow secondary motor neurons but not in primary, or fast and intermediate secondary motor neurons (B, C). In the cerebellum, *pcdh9* positive cells were positive for ZebrinII both in the valvula lateralis (Val) and valvula medialis (Vam) (D) and in the corpus cerebelli (CCe) (E). Scale bars equal 20 μm.

inhibitory interneurons and motor neurons, recruited sequentially at slow, intermediate, and fast swim frequencies (Ampatzis et al., 2014). We found overlap with *pcdh9* for all these types of neurons; leaving the door open to the possibility of a distinct neuronal network. Having shown expression in slow motor neurons, this *pcdh9* reporter line provides an ideal starting point to test if protocadherins could be an essential part in establishing these distinct neuronal circuits. Electrophysiological experiments such as double patch-clamping of eGFP positive neurons or tracing approaches, using a retrograde/anterograde synapse-jumping virus, should be performed to offer direct evidence for connections between *pcdh9*:hs:eGFP labelled cells.

4. Material and methods

4.1. Animals

Adult zebrafish (Ab strain) were housed at the Genome Engineering Zebrafish National Facility (SciLife Lab, Uppsala, Sweden) under standard conditions of 14/10 h light/dark cycles at 28 °C. Appropriate ethical approvals were obtained from a local ethical board in Uppsala (C164/14 and 14088/2019) and Karolinksa Institutet, Stockholm (9248-2017 and 19535-2020).

The transgenic lines Tg(*dmrt3a*:GAL4; UAS:RFP) (Satou et al., 2020) and Tg(*mnx1*:Gal4; UAS:RFP) (Seredick et al., 2012), Tg(*HuC*:GAL4; UAS:RFP) (Park et al., 2000) and Tg(*ptf1a*:dsred) (Boije et al., 2015) were used in crosses with the new Tg(*pcdh9*:hs:eGFP) zebrafish. Embryos and larvae were kept at 28 °C. To prevent pigmentation, 1-Phenyl-2-thiourea (PTU, 0.003% final concentration) was added at 24 h post fertilisation (hpf).

4.2. CRISPR/Cas9 knock in

We inserted a plasmid containing eGFP driven by a minimal heat shock promoter upstream of the 5′UTR of *pcdh9* (Fig. 1A). With a specific guide RNA we targeted DNA 88 basepairs upstream of the start of the 5′UTR of *pcdh9* and Cas9 introduces a double strand break and by non-homologous end joining the eGFP will be inserted and its expression is regulated by the same machinery as the expression of the gene of interest. Knock-in experiments were based on a previously published method (Kimura et al., 2015). Two CRISPR targets were designed within 100bp upstream of the 5′UTR of *pcdh9* using CRISPor and ChopChop (transcript: ENSDART00000186730.1). Target 1: ZNN-25 pcdh9 GCGGAGAGGGCGTTCCCTGT (predicted score: Moreno 79, Doench 52) and target 2: ZNN-26 pcdh9 GGGCGGGGGAATAATGCGAT (predicted score: Moreno 88, Doench 49). Using the oligo assembly approach to prepare sgRNAs (Varshney et al., 2015) we synthetically added a G to the target ZNN-25 GGGAGAGGGCGTTCCCTGT since this is crucial for the T7 polymerase. Oligos were ordered with a T7 promoter 5′ of the target sequence and a DNA stretch overlapping with the guide core sequence at the 3′ end (for ZNN-25 taatacgactcactataGGGAGAGGGCGTTCCCTGTgttttagagctagaaatagcaag, for ZNN-26 taatacgactcactataGGGCGGGGGAATAATGCGATgttttagagctagaaatagcaag). The oligos were then annealed with a second fragment containing the guide core sequence (oligoB) (Varshney et al., 2015). The same principle was used for the oligo to generate the sgRNA to cut the mbait sequence in the plasmid (taatacgactcactataGGCTGCTGCGGTTCCAGAGGgttttagagctagaaatagcaag). These products were then used as a template for RNA in vitro transcription (HiScribe T7 High Yield RNA Synthesis Kit, NEB) and the generated RNA was purified prior to injection. To prepare Cas9 mRNA, pT3Ts-nCas9 plasmid (Addgene 46757) was digested with

Xba1 (NEB), purified and used for T3 driven in vitro transcription according to the manual provided by the manufacturer (mMESSAGE m MACHINE T3 Kit, Life Technologies).

4.3. Injections

Fertilized zebrafish eggs from AB fish were obtained in natural crosses, injected at the one-cell stage into the cell with 110 pg of Cas9 mRNA, 250 pg Cas9 protein (TrueCut™ Cas9 Protein V2, Invitrogen), 50 pg of sgRNA for gene specific target and 50 pg of mbait sgRNA and 1,5 pg of the mbait-hs-eGFP plasmid (kindly provided by Professor Atsuo Kawahara (Ota et al., 2016). eGFP positive larvae were raised and outcrossed with AB confirm for germline transmission.

4.4. Assessing sgRNA efficiency by fluorescent PCR

DNA of injected embryos was extracted at 3dpf by dissolving tissue in 30 μl 50 mM NaOH for 20 min in 95 °C, adding 60 μl 50 mM Tris-HCl. A 3-primer-PCR was performed with pcdh9 forward primer tgtaaaacgacggccagtTGAAATGGAACCGTACATTGAG, pcdh9 reverse primer gtgtcttGTGAGATGTGTTGGGATGCTTA and M13 forward primer (TGTAAAACGACGGCCAGT) fluorescently labelled with 6-FAM (Varshney et al., 2015). PCR products were analysed by fragment separation using capillary electrophoresis (or fragment length analysis), as previously described (Sood et al., 2013). Size determination was carried out on a 3130XL ABI Genetic Analyzer (Applied Biosystems, Waltham, MA) and the data was analysed using the Peak Scanner Software (Thermo Fisher Scientific, Waltham, MA). The length of the fragments was compared to the WT product length, predicted by in silico PCR using the USCS browser. More fragments (peaks) were found for target ZNN25, considered higher efficient and therefore used for injections.

4.5. Sequencing

The pcdh9 forward primer used for the fluorescent PCR was reused in combination with a reverse primer in the heat shock promoter sequence GCCCGTCTGTTCATTGTTTT. PCR products were cleaned with PCR Clean up Kit (Qiagen) and sequenced from M13. This confirmed genomic position of the insert at the right location and that the insert was integrated in a forward direction.

4.6. Whole mount immunohistochemistry

4.6.1. Larvae

Zebrafish larvae were fixed at 3 dpf in 4% paraformaldehyde for 15 min at room temperature (RT). Embryos were washed (PBST (0.1%T)), cryoprotected (30% sucrose 2h RT) and treated with Aceton for 20 min in −20 °C. Blocking was done with 1% BSA in PBS for 1h at RT prior to primary antibody incubation diluted in 1% BSA in 4 °C overnight. Primary antibodies used: mouse anti-Wt1 1:100 from Dako, chicken anti-GFP 1:1000 from Aves Lab, rabbit anti-Evx2 1:3000, a gift from Shinichi Higashijima, mouse anti-Isl1/2 (in text referred to as Isl1) 1:200 from Hybridoma Bank. Next larvae were washed (PBST (0.1%T) 2 × 1h) and incubated with their respective secondary antibody overnight at 4 °C. Secondary antibodies used: FITC goat anti-chicken (1:500), Alexa Fluor 594 donkey anti-mouse (1:1500), Alexa Fluor 647 donkey anti-rabbit (1:500). Finally, the larvae were washed (PBST (0.1%T) 2 × 1h) and imaged.

4.6.2. Juveniles

Juvenile zebrafish (6–8 weeks old) were deeply anesthetized with tricaine methane sulfonate (MS-222, Sigma-Aldrich, E10521). The spinal cord and the brain were extracted and fixed in 4% paraformaldehyde (PFA) and 5% saturated picric acid (Sigma-Aldrich, P6744) in PBS (0.01 M; pH = 7.4, Santa Cruz Biotechnology, Inc., CAS30525-89-4) at 4 °C overnight. Immunolabeling was performed both in whole-mount spinal cords and on brain cryosections. For sections, the tissue was removed carefully and cryoprotected overnight in 30% (w/v) sucrose in PBS at 4 °C, embedded in Cryomount (Histolab, 45830) sectioning medium, rapidly frozen in dry-ice-cooled isopentane (2-methylbutane; Sigma-Aldrich, 277258) at approximately −35 °C, and stored at −80 °C until use. Transverse coronal plane cryosections (thickness: 25 μm) of the tissue were collected and processed for immunohistochemistry. For all sample types (whole-mount and cryosections), the tissue was washed 3 times for 5 min each in PBS. Nonspecific protein binding sites were blocked with 4% normal donkey serum (NDS; Sigma-Aldrich, D9663) with 1% BSA (Sigma-Aldrich, A2153) and 1% Triton X-100 (Sigma-Aldrich, T8787) in PBS for 1h at RT. Primary antibodies: mouse anti-HuCD monoclonal 16A11 (1:500, Invitrogen, A-21271), chicken anti-GFP (1:500, abcam, 13970), mouse anti-ZebrinII (1:400, a kind gift from Richard Hawkes, ACHR, University of Calgary, Calgary, AB, Canada) were diluted in 1% of the blocking solution and applied for 1–3 days at 4 °C. After thorough buffer rinses, the tissues were then incubated with the appropriate secondary antibodies diluted with streptavidin conjugated to Alexa Fluor 568 or Alexa Flour 647 (1:500, ThermoFisher, S32357) in 1% Triton X-100 (Sigma-Aldrich, T8787) in PBS overnight at 4 °C. Finally, the tissue was thoroughly rinsed in PBS and cover-slipped with a hard fluorescent medium (VectorLabs; H-1400).

4.7. Motor neuron labelling

Retrograde labelling of motor neurons was performed in anesthetized zebrafish with 0.03% tricaine by using dye injection with biotinylated dextran (3000 molecular weight, D7135; Thermo Fisher) into all muscles of myotomes 14–16, and let to recover overnight to allow the retrograde transport of the tracer.

4.8. Imaging

A Leica SP8 (Leica Microsystems, Wetzlar, Germany) confocal microscope with an additional DLS (Digital Light Sheet) module and a Zeiss LSM 800 confocal microscope was used for imaging. Living larvae were anesthetized by Tricaine (0.12 mg/ml) and both living and fixed larvae were mounted in low melting agarose (1.2% for confocal microscopy; 0.8% for light sheet microscopy). Image processing was done in LasX, ZEN software and Fiji.

Declaration of competing interest

The authors declare that there is no conflict of interest.

Acknowledgement

We thank the Genome Engineering Zebrafish National Facility, Uppsala, Sweden for fish husbandry, and input and exchange of method development. We thank Professor Atsuo Kawahara and Professor Shinichi Higashijima for providing the mbait-hs-eGFP plasmid and the Evx2 antibody. This work has been financially supported by grants from the following foundations: the Kjell and Marta Beijers Foundation; the Jeanssons foundation; the Carl Tryggers Foundation; the Swedish Brain Foundation; the Swedish Research Council; the Magnus Bergvalls Foundation, the Royal Swedish Academy of Sciences; the Ake Wibergs Foundation; Olle Engkvist Stiftelse; the Ragnar Soderberg Foundation, Swedish Foundation for Strategic Research, NARSAD-Brain, Behavior Research Foundation (26004) and Swedish Research Council (2015–03359 and 2020-00943).

Appendix A. Supplementary data

Supplementary data to this article can be found online at https://doi.org/10.1016/j.gep.2022.119246.

References

Alaynick, W.A., Jessell, T.M., Pfaff, S.L., 2011. SnapShot: spinal cord development. Cell 146 (1). https://doi.org/10.1016/j.cell.2011.06.038.

Ampatzis, K., et al., 2013. Pattern of innervation and recruitment of different classes of motoneurons in adult zebrafish. J. Neurosci. 33 (26) https://doi.org/10.1523/JNEUROSCI.0896-13.2013.

Ampatzis, K., et al., 2014. Separate microcircuit modules of distinct V2a interneurons and motoneurons control the speed of locomotion. Neuron 83 (4), 934–943. https://doi.org/10.1016/j.neuron.2014.07.018.

Andersson, L.S., et al., 2012. Mutations in DMRT3 affect locomotion in horses and spinal circuit function in mice. Nature 488 (7413). https://doi.org/10.1038/nature11399.

Asahina, H., et al., 2012. Distribution of protocadherin 9 protein in the developing mouse nervous system. Neuroscience 225, 88–104. https://doi.org/10.1016/J.NEUROSCIENCE.2012.09.006.

Bae, Y.-K., et al., 2009. Anatomy of zebrafish cerebellum and screen for mutations affecting its development. Dev. Biol. 330 (2) https://doi.org/10.1016/j.ydbio.2009.04.013.

Bello-Rojas, S., et al., 2019. Central and peripheral innervation patterns of defined axial motor units in larval zebrafish. J. Comp. Neurol. 527 (15) https://doi.org/10.1002/cne.24689.

Berg, E.M., et al., 2018. Principles governing locomotion in vertebrates: lessons from zebrafish. Front. Neural Circ. 12 https://doi.org/10.3389/fncir.2018.00073.

Boije, H., et al., 2015. The independent probabilistic firing of transcription factors: a paradigm for clonal variability in the zebrafish retina. Dev. Cell 34 (5). https://doi.org/10.1016/j.devcel.2015.08.011.

Boije, H., et al., 2016. Horizontal cells, the odd ones out in the retina, give insights into development and disease. Front. Neuroanat. 10 https://doi.org/10.3389/fnana.2016.00077.

Comer, J.D., et al., 2015. Sensory and spinal inhibitory dorsal midline crossing is independent of Robo3. Front. Neural Circ. 9 https://doi.org/10.3389/fncir.2015.00036.

Fontenas, L., Kucenas, S., 2018. Motor Exit point (MEP) glia: novel myelinating glia that bridge CNS and PNS myelin. Front. Cell. Neurosci. 12 https://doi.org/10.3389/fncel.2018.00333.

Frank, M., Kemler, R., 2002. Protocadherins. Curr. Opin. Cell Biol. 14 (5) https://doi.org/10.1016/S0955-0674(02)00365-4.

Goulding, M., 2009. Circuits controlling vertebrate locomotion: moving in a new direction. Nat. Rev. Neurosci. 10 (7) https://doi.org/10.1038/nrn2608.

Hale, M.E., Ritter, D.A., Fetcho, J.R., 2001. A confocal study of spinal interneurons in living larval zebrafish. J. Comp. Neurol. 437 (1) https://doi.org/10.1002/cne.1266.

Hamling, K.R., Tobias, Z.J.C., Weissman, T.A., 2015. Mapping the development of cerebellar Purkinje cells in zebrafish. Devel. Neurobiol. 75 (11) https://doi.org/10.1002/dneu.22275.

Henderson, K.W., Menelaou, E., Hale, M.E., 2019. Sensory neurons in the spinal cord of zebrafish and their local connectivity. Curr Opin Physiol 8. https://doi.org/10.1016/j.cophys.2019.01.008.

Hoshino, M., et al., 2005. Ptf1a, a bHLH transcriptional gene, defines GABAergic neuronal fates in cerebellum. Neuron 47 (2). https://doi.org/10.1016/j.neuron.2005.06.007.

Iglesias Gonzalez, A., et al., 2021. Single cell transcritpomic analysis of spinal Dmrt3 neurons in zebrafish and mouse identifies distinct subtypes and reveal novel subpopulations within the dI6 domain. Front. Cell. Neurosci. 15, 781197. https://doi.org/10.3389/fncel.2021.781197.

Iribarne, M., 2020. Zebrafish photoreceptor degeneration and regeneration Research to understand hereditary human blindness. In: Visual Impairment and Blindness - what We Know and what We Have to Know. IntechOpen. https://doi.org/10.5772/intechopen.88758.

Iwasaki, M., et al., 2020. Development of the anterior lateral line system through local tissue-tissue interactions in the zebrafish head. Dev. Dynam. 249 (12) https://doi.org/10.1002/dvdy.225.

Jusuf, P.R., Harris, W.A., 2009a. Ptf1a is expressed transiently in all types of amacrine cells in the embryonic zebrafish retina. Neural Dev. 4 (1) https://doi.org/10.1186/1749-8104-4-34.

Jusuf, P.R., Harris, W.A., 2009b. Ptf1a is expressed transiently in all types of amacrine cells in the embryonic zebrafish retina. Neural Dev. 4 (1) https://doi.org/10.1186/1749-8104-4-34.

Kimura, Y., et al., 2015. Efficient generation of knock-in transgenic zebrafish carrying reporter/driver genes by CRISPR/Cas9-mediated genome engineering. Sci. Rep. 4 (1) https://doi.org/10.1038/srep06545.

Lencer, E., Prekeris, R., Artinger, K.B., 2021. Single-cell RNA analysis identifies pre-migratory neural crest cells expressing markers of differentiated derivatives. Elife 10. https://doi.org/10.7554/eLife.66078.

Li, X., et al., 2012. Pineal photoreceptor cells are required for maintaining the circadian rhythms of behavioral visual sensitivity in zebrafish. PLoS One 7 (7). https://doi.org/10.1371/journal.pone.0040508.

Lin, J., Wang, C., Redies, C., 2012. Expression of delta-protocadherins in the spinal cord of the chicken embryo. J. Comp. Neurol. 520 (7) https://doi.org/10.1002/cne.22808.

Liu, Q., et al., 2009. Expression of protocadherin-9 and protocadherin-17 in the nervous system of the embryonic zebrafish. Gene Expr. Patterns 9 (7). https://doi.org/10.1016/j.gep.2009.07.006.

Masai, I., et al., 1997. Floating head and masterblind regulate neuronal patterning in the roof of the forebrain. Neuron 18 (1). https://doi.org/10.1016/S0896-6273(01)80045-3.

McGraw, H.F., et al., 2012. Postembryonic neuronal addition in Zebrafish dorsal root ganglia is regulated by Notch signaling. Neural Dev. 7 (1) https://doi.org/10.1186/1749-8104-7-23.

McGraw, H.F., Nechiporuk, A., Raible, D.W., 2008. Zebrafish dorsal root ganglia neural precursor cells adopt a glial fate in the absence of Neurogenin1. J. Neurosci. 28 (47) https://doi.org/10.1523/JNEUROSCI.2079-08.2008.

Medina, J.F., 2011. The multiple roles of Purkinje cells in sensori-motor calibration: to predict, teach and command. Curr. Opin. Neurobiol. 21 (4) https://doi.org/10.1016/j.conb.2011.05.025.

Moran-Rivard, L., et al., 2001. Evx1 is a postmitotic determinant of V0 interneuron identity in the spinal cord. Neuron 29 (2). https://doi.org/10.1016/S0896-6273(01)00213-6.

Morris, A.D., Lewis, G.M., Kucenas, S., 2017. Perineurial glial plasticity and the role of TGF-β in the development of the blood–nerve barrier. J. Neurosci. 37 (18) https://doi.org/10.1523/JNEUROSCI.2875-16.2017.

Nicolson, T., 2005. The genetics of hearing and balance in zebrafish. Annu. Rev. Genet. 39 (1) https://doi.org/10.1146/annurev.genet.39.073003.105049.

Ota, S., et al., 2016. Functional visualization and disruption of targeted genes using CRISPR/Cas9-mediated eGFP reporter integration in zebrafish. Sci. Rep. 6 (1) https://doi.org/10.1038/srep34991.

Pancho, A., et al., 2020. Protocadherins at the crossroad of signaling pathways. Front. Mol. Neurosci. 13 https://doi.org/10.3389/fnmol.2020.00117.

Park, H.-C., et al., 2000. Analysis of upstream elements in the HuC promoter leads to the establishment of transgenic zebrafish with fluorescent neurons. Dev. Biol. 227 (2), 279–293. https://doi.org/10.1006/dbio.2000.9898.

Peek, S.L., Mah, K.M., Weiner, J.A., 2017. Regulation of neural circuit formation by protocadherins. Cell. Mol. Life Sci. 74 (22) https://doi.org/10.1007/s00018-017-2572-3.

Sellick, G.S., et al., 2004. Mutations in PTF1A cause pancreatic and cerebellar agenesis. Nat. Genet. 36 (12) https://doi.org/10.1038/ng1475.

Seredick, S.D., et al., 2012. Zebrafish Mnx proteins specify one motoneuron subtype and suppress acquisition of interneuron characteristics. Neural Dev. 7 (1) https://doi.org/10.1186/1749-8104-7-35.

Shainer, I., et al., 2017. Novel hypophysiotropic AgRP2 neurons and pineal cells revealed by BAC transgenesis in zebrafish. Sci. Rep. 7 (1) https://doi.org/10.1038/srep44777.

Sood, R., et al., 2013. Efficient methods for targeted mutagenesis in zebrafish using zinc-finger nucleases: data from targeting of nine genes using CompoZr or CoDA ZFNs. PLoS One 8 (2). https://doi.org/10.1371/journal.pone.0057239.

Vanhalst, K., et al., 2005. δ-Protocadherins: a gene family expressed differentially in the mouse brain. Cell. Mol. Life Sci. CMLS 62 (11). https://doi.org/10.1007/s00018-005-5021-7.

Varshney, G.K., et al., 2015. High-throughput gene targeting and phenotyping in zebrafish using CRISPR/Cas9. Genome Res. 25 (7) https://doi.org/10.1101/gr.186379.114.

Wada, H., et al., 2013. Innervation is required for sense organ development in the lateral line system of adult zebrafish. Proc. Natl. Acad. Sci. Unit. States Am. 110 (14) https://doi.org/10.1073/pnas.1214004110.

Xiao, Y., et al., 2015. High-resolution live imaging reveals axon-glia interactions during peripheral nerve injury and repair in zebrafish. Dis Model Mech 8 (6), 553–564. https://doi.org/10.1242/dmm.018184.